The Second International Symposium on Atomic Technology IOP Publishing
Journal of Physics: Conference Series **106** (2008) 012001 doi:10.1088/1742-6596/106/1/012001

Diffusion and Ionic Conduction in Oxide Glasses

Helmut Mehrer, Arpad W. Imre[1] and Eugene Tanguep-Nijokep[1]

Institut für Materialphysik, Universität Münster, Wilhelm-Klemm-Str. 10, 48149 Münster, Germany and Sonderforschungsbereich 458, Universität Münster, Germany

E-mail: mehrer@uni-muenster.de

Abstract. The ion transport properties of soda-lime silicate and alkali borate glasses have been studied with complimentary tracer diffusion and impedance spectroscopy techniques in order to investigate the ion dynamics and mixed-alkali effect (MAE). In soda-lime silicate glasses the tracer diffusivity of ^{22}Na alkali ions is more than six orders of magnitude faster than the diffusivity of earth alkali ^{45}Ca ions. This observation is attributed to a stronger binding of bivalent earth alkali ions to the glass network as compared to that of alkali ions. The conductivity of the investigated standard soda-lime silicate glasses is mostly due to the high mobility of sodium ions and a temperature independent Haven ratio of about 0.45 is obtained. For single alkali sodium-borate glasses, the Haven ratio is also temperature independent, however, it is decreases with decreasing temperature for rubidium-borate glass. The MAE was investigated for Na-Rb borate glasses and it was observed that the tracer diffusivities of ^{22}Na and ^{86}Rb ions cross, when plotted as function of the relative alkali content. This crossover occurs near the Na/(Na+Rb) ratio of the conductivity minimum due to MAE. The authors suggest that this crossover and the trend of diffusion coefficients is the key to an understanding of the MAE.

1. Introduction

Glasses are formed in a great variety of systems including manmade and natural glasses. Oxide glasses are the best known class of non-crystalline materials and comprise a large number of glass families. The crystallography, chemistry and physics of glasses encompasses a vast body of information. We refer the interested reader to textbooks on glass [1 - 4]. Oxide glasses are network glasses and are composed of network formers and network modifiers. In our case the network formers are SiO_2 or B_2O_3 and the network modifiers are alkali oxides and/or earth-alkaline oxides. Our glasses, like many other oxide glasses, are ionic conductors. Fundamentals of tracer diffusion and ionic conduction can be found, e.g., in a recent textbook by one of the present authors [5].

In the present paper we summarize some typical results about tracer diffusion and ionic conduction in soda-lime silicate glass and single-alkali and mixed-alkali borate glass obtained in our laboratory. We have studied tracer diffusion of modifier cations and ionic conduction as functions of composition, temperature and, in the case of borate glass, also of pressure. Here we give a brief account of the temperature and composition dependence of tracer diffusion and of ionic conduction. Details can be found for soda-lime glasses in [6, 7] and for alkali-borate glasses in [8 - 19]. Pressure effects, which are not considered in the present paper, are discussed for single-alkali borate glass in [20].

[1] Present address: Institut für Physikalische Chemie, Universität Münster, Corrensstr. 28/30, 48149 Münster, Germany

2. Soda-lime silicate glass

2.1. Composition and structure

Soda-lime silicate glasses contain mainly sodium and calcium oxides as network modifiers and silica as network former. Soda-lime glasses are perhaps the least expensive and most widely used of all the glasses made commercially. Most of the glass of windows, beverage bottles, and envelopes of incandescent and fluorescent lamps are made from soda-lime glass.

The structure of a soda-lime glass is conveniently described by the rules of ZACHARIASEN (see, e.g., [1, 5]). The silicon-oxygen tetrahedron is the network former and serves as the basic building block of the glass network. If modifier cations are introduced, by melting Na_2O and CaO together with SiO_2, some Si-O-Si bridges are broken. Then oxygen atoms occupy free ends of separated tetrahedra and form non-bridging oxygen (NBO) units. The NBO units are the anionic counterparts of the Na and Ca cations. The modifier cations (Na^+ and Ca^{2+}) are mainly incorporated at the severance sites of the silica network. This structure provides a stronger linkage of the network to the divalent alkaline-earth ions than to the monovalent alkali ions. Thus, the Na ions are considerably more mobile than the Ca ions.

We have studied glasses which had been produced by the Deutsche Glastechnische Gesellschaft as standard glasses for physical and chemical testing. In what follows we illustrate typical results for a glass composed of about 72.3 % of SiO_2, 13.6 % of Na_2O, 6.8 % of CaO, 5.9 % of MgO and some further but minor additions.

2.2. Tracer diffusion, charge diffusion and viscosity diffusion

The diffusion of the radioisotopes ^{22}Na and ^{45}Ca was monitored by the radiotracer technique in combination with grinder or sputter sectioning (for details see, e.g., [5]). Examples of penetration profiles for ^{45}Ca in soda-lime glass are displayed in Fig. 1. Diffusion was studied below and above the calorimetric glass-transition temperature. The profiles of Fig. 1 pertain to diffusion anneals in the supercooled glass melt.

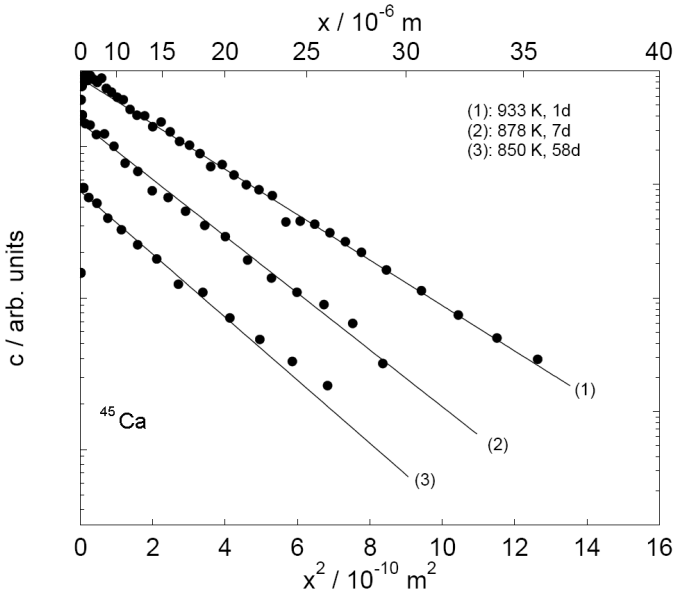

Figure 1. Examples for penetration profiles of ^{45}Ca in soda-lime glass.

Solid lines in Fig. 1 illustrate the thin-film solution of Fick's second law:

$$C(x,t) \;=\; \frac{M}{\sqrt{\pi D^* t}} \exp\left(-\frac{x^2}{4D^* t}\right). \qquad (1)$$

In eqn. (1) D^* denotes the tracer diffusivity, t the duration of the diffusion anneal, and M the amount of tracer deposited as thin film onto the sample surface. A fit of eqn. (1) to the data

permits to deduce the Ca diffusivity. Tracer diffusion coefficients of Na have been deduced in the same way.

As already mentioned oxide glasses are ion conductors. We have studied the ionic conductivity of soda-lime glass by impedance spectroscopy (for details see, e.g., [5, 21]). The conductivity as function of the frequency for various temperatures is shown in Fig. 2. The low-frequency plateau corresponds to the dc-conductivity σ_{dc}. It reflects the long-range transport of mobile ions in the glass. The conductivity dispersion at higher frequencies is due to correlated forward and backward hops of ions (see, e.g., [22]). The disperion contains useful information as well, which, however, is not considered here.

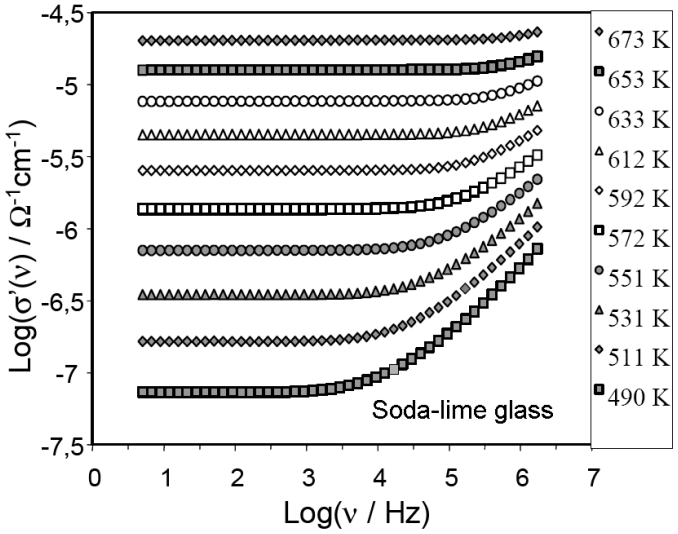

Figure 2. Conductivity spectra of a soda-lime silicate glass.

The diffusivities of both network-modifier ions are displayed in the Arrhenius diagram of Fig. 3 together with further transport properties discussed below. The tracer diffusivities of Na are many orders of magnitude higher than those of Ca. This confirms the view mentioned above that Ca has a stronger binding to the network.

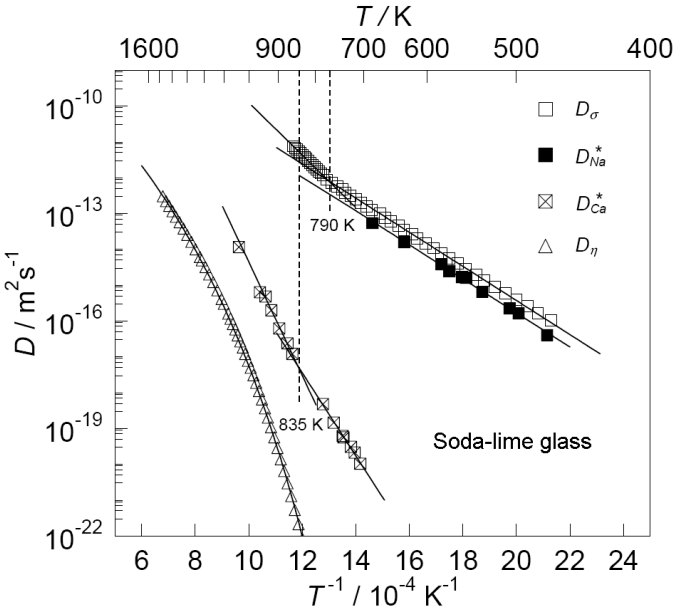

Figure 3. Arrhenius diagram of the tracer diffusivities of ^{22}Na and ^{45}Ca, of the charge diffusion coefficient D_σ, and of the viscosity diffusion coefficient D_η for a soda-lime silicate glass. The dashed lines indicate the glass-transition region.

By implying the *Nernst-Einstein relation* it is common practice in the solid-state diffusion

literature to deduce the so-called *charge diffusion coefficient* D_σ (see, e.g., [5]) from the dc-conductivity via

$$D_\sigma = \frac{\sigma_{dc} k_B T}{q^2 N_{ion}}. \quad (2)$$

Here k_B denotes the Boltzmann constant, T the absolute temperature, and N_{ion} the number density of mobile ions. One should, however, keep in mind that D_σ is not a diffusion coefficient that can be measured by way of Fick's laws.

In eqn. (2) we used the number density of Na ions, which is known from the glass composition. This appears to be well justified by the tracer data, which show that the mobility of Ca ions is negligible as compared to that of Na ions. Fig. 3 shows that the charge diffusivity is only slightly higher than the tracer diffusivity of Na ions. In addition, the fact that conductivity diffusion and tracer diffusion of Na have practically the same activation enthalpy enforces the conclusion that the ionic conductivity of soda-lime glass is due to the motion of Na ions.

The ratio between tracer diffusivity and charge diffusivity

$$H_R = \frac{D^*}{D_\sigma} \quad (3)$$

is denoted as the *Haven ratio*. The Haven ratio contains information about the correlation and the collectivity of the atomic mechanism of ionic motion. For our soda-lime glass the Haven ratio equals about 0.45 and is practically independent of temperature. This indicates that the mechanism of Na diffusion does not change with temperature.

The viscosity η is a property which measures the resistance of a melt or of an undercooled melt to shear deformation and is a very important property in glass technology. It plays a significant role in all stirring processes, in the buoyancy of bubbles during glass fining processes, during glass formation, and for nucleation and growth of crystalline phases. A glass-forming melt acts as a liquid at high temperatures and turns into a glassy solid upon cooling below the glass-transition region. The viscosity of soda-lime glass has been measured over many orders of magnitude at the Physikalisch Technische Bundesanstalt (Braunschweig, Germany). The *Stokes-Einstein equation* relates the viscosity to the so-called *viscosity diffusion coefficient* D_η (see, e.g., [5]) via

$$D_\eta = \frac{k_B T}{6\pi r \eta}. \quad (4)$$

r is some characteristic radius. The viscosity diffusion coefficient calculated from viscosity data assuming for r the radius of the $SiO_{4/2}$ unit is displayed in Fig. 3. The viscosity diffusivity can be well described by Vogel-Fulcher-Tammann behaviour (see, e.g., [5]). Its temperature dependence is decidedly non-Arrhenian. The viscosity and hence D_η are somehow characteristic for the mobility of the network-forming units. In the undercooled melt and in the glassy state the tracer diffusivities of Na are decoupled from the much slower motion of the network-forming units. To some extent this statement holds for the Ca diffusivities as well.

3. Borate glass

3.1. Structure and composition

The structure of borate (B_2O_3) differs considerably from that of SiO_2. Only the triangular coordination is formed in vitreous B_2O_3. The $BO_{3/2}$ units are connected at all three corners via B-O-B bonds to form a network. A three-dimensional random structure is obtained by 'crumpling' the network. The addition of alkali oxides to B_2O_3 forces some of the boron to change from trigonal to tetrahedral coordination. The formation of two boron-oxygen tetrahedra consumes the additional oxygen provided by one alkali oxide molecule. The as-formed tetrahedrally coordinated $BO^-_{4/2}$ units form the anionic counterparts of the alkali ions. Each Na_2O or Rb_2O molecule creates two $BO^-_{4/2}$ units. The glass-transition temperature of alkali borate glasses increases upon addition

of alkali oxide as the three-dimensional connectivity increases. Only at concentrations larger than about 25 % alkali oxide NBO units are also formed.

The alkali borate glasses were prepared in our laboratory from dried powders of B_2O_3 and Na_2CO_3 or/and Rb_2CO_3. The powders were melted together in a platinum crucible at about 1273 K, where CO_2 bubbles off from the melt. The melt is then poured into a stainless steel container to form a glassy rod. In this way single-alkali glasses and mixed-alkali glasses $Y[XNa_2O(1-X)Rb_2O](1-Y)B_2O_3$ with $Y=$ 0.2 and 0.3 were obtained. Na borate glass corresponds to $X=1$ and Rb borate glass to $X=0$. Mixed-alkali glasses correspond to X-values between 1 and 0.

3.2. Tracer diffusion and ionic conductivity in alkali borate glass

In this section we report typical results for Na borate glass and for Rb borate glass. We have studied the diffusion of the radioisotopes ^{22}Na and ^{86}Rb by the radiotracer technique in combination with either grinder or sputter sectioning (for details see, e.g., [5]). Examples of penetration profiles for both isotopes are displayed in Fig. 4. Solid lines illustrate the thin-film solution of Fick's second law eqn. (1). The penetration profiles are described by the thin-film solution over several orders of magnitude.

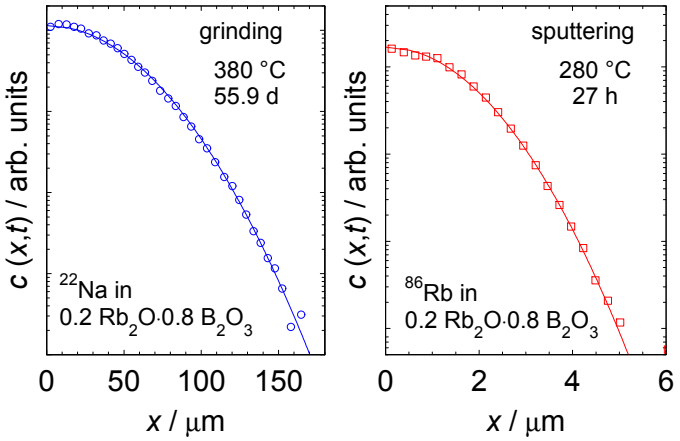

Figure 4. Examples of penetration profiles of ^{22}Na and of ^{86}Rb in rubidium borate glass.

We also studied the ionic conductivity by impedance spectroscopy. Examples of the conductivity (times absolute temperature) as function of the frequency are shown in Fig. 5. The low-frequency plateau corresponds to the dc-conductivity σ_{dc}. The dc-conductivity reflects the long-range transport of mobile Na ions in the glass and is Arrhenius activated. In the Arrhenius diagrams of Figs. 6 and 7 we compare the tracer diffusivity of ^{22}Na in Na borate glass and that of ^{86}Rb in Rb borate glass with the corresponding charge diffusivity calculated from the dc-conductivities via eqn. (2).

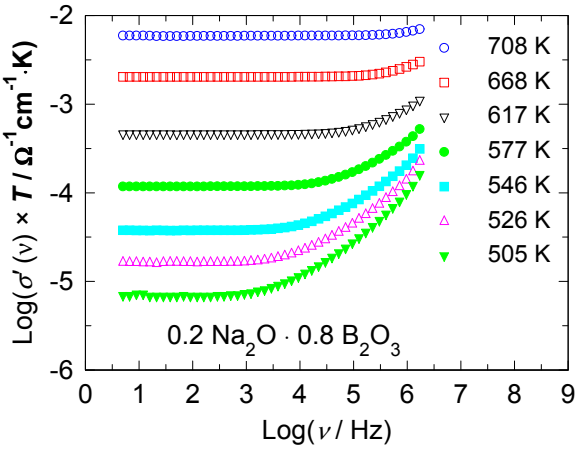

Figure 5. Conductivity spectra of a sodium borate glass.

For the sodium borate glass the tracer diffusion coefficient and the charge diffusivity have the same activation enthalpy. This is equivalent with the statement that the Haven ratio is independent of temperature. This fact implies that the atomic mechanism of Na diffusion does not change. This is in remarkable contrast to the findings for rubidium borate glass. Here the activation enthalpies of tracer and charge diffusion are different. The Haven ratio decreases with decreasing temperature with an activation enthalpy of about 20.9 kJ mol^{-1}.

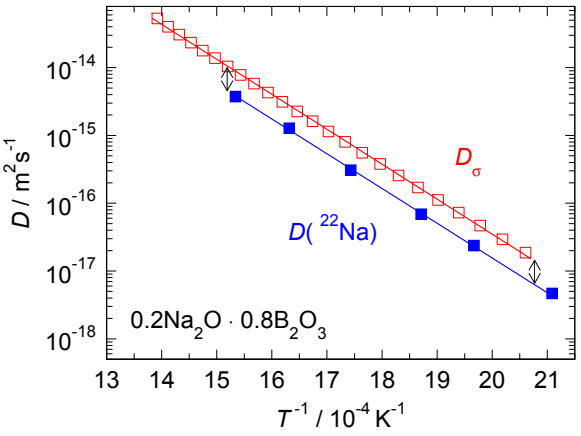

Figure 6. Arrhenius diagram of the tracer diffusivity of ^{22}Na and of the charge diffusion coefficient D_σ for a sodium borate glass.

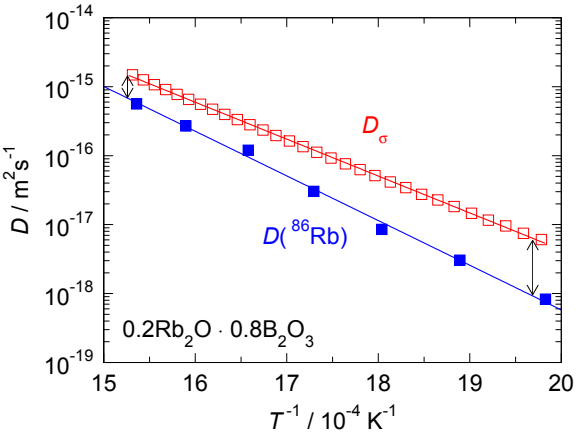

Figure 7. Arrhenius diagram of the tracer diffusivity of ^{86}Rb and of the charge diffusion coefficient D_σ for a rubidium borate glass.

In addition, in our high pressure experiments we found that the Haven ratio for rubidium borate glass decreases with increasing pressure by about a factor of 10 between ambient pressure and 6 kbar, whereas the Haven ratio of the sodium borate glass is almost pressure independent [20]. This finding was attributed to a collective mechanism of ionic motion in borate glass. The ions move in a caterpillar-like fashion in a more or less curled chain of ions. Each jump of a mobile ion can be considered as a step promoted by a 'vacancy-like' defect moving in this chain. The jumping tracer atom in such a chain is responsible for diffusion, whereas the charge diffusion can be attributed to the motion of the 'vacancy-like' defects. The 'vacancies' can be considered as the carriers of charge. Their motion is highly correlated. For rubidium borate glass the degree of collectivity changes with pressure and temperature. Increasing pressure and decreasing temperature enhances the degree of collectivity in the caterpillar-like motion of ions, because motion in more stretched chains has lower activation barriers than out-of-chain hops. This entails a temperature and pressure dependent Haven ratio [20].

3.3. Mixed-alkali effect

Oxide glasses which contain two alkali oxides can reveal the so-called mixed-alkali effect (MAE), which is a long-known but still very interesting feature of ionic conduction and diffusion in glass. If the total content of two alkali oxides is kept constant but the ratio of the different alkali ions is varied, the conductivity passes through a deep minimum. Fig. 8 shows typical examples. If Na ions are gradually replaced by Rb ions the conductivity does not at all follow a linear mixing rule as one perhaps might expect. For this particular glass system a minimum occurs near about 40 % Na/(Na +Rb) ratio. The depth of the MAE minimum increases with decreasing temperature. As a consequence the activation enthalpy of the conductivity passes through a maximum at an intermediate composition. Conductivity minima are perhaps the best-known fingerprints of the mixed-alkali effect. Many further examples can be found in the literature (see, e.g., [23, 24]). We also note, without further discussion, that the mixed-alkali effect decreases with decreasing total alkali content and vanishes for low contents [12].

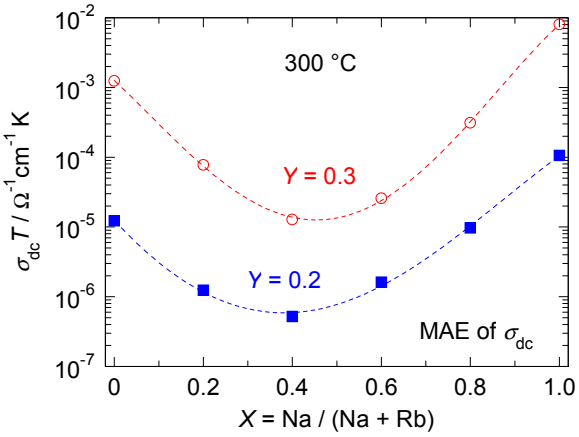

Figure 8. Mixed-alkali effect (MAE) of the dc-conductivity (times temperature) for two series of $Y[X\mathrm{Na_2O}(1-X)\mathrm{Rb_2O}](1-Y)\mathrm{B_2O_3}$ glasses.

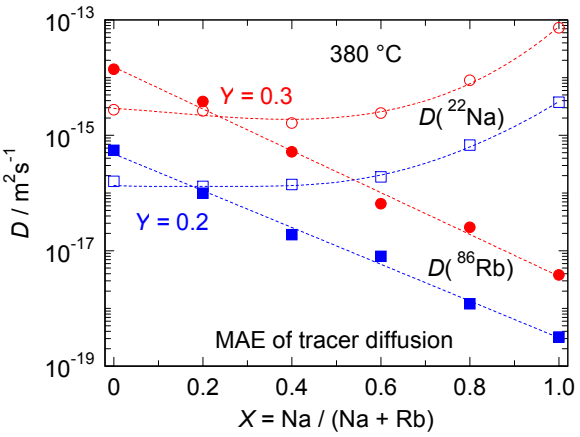

Figure 9. Mixed-alkali effect (MAE) of ^{22}Na and ^{86}Rb tracer diffusion in two series of Na-Rb borate glasses.

Systematic studies of alkali tracer diffusion in mixed-alkali glasses are relatively rare because tracer studies are laborious and time-consuming (see, e.g., [5]). We have performed such studies for a series of mixed Na-Rb borate glasses. Fig. 9 displays typical results and reveals significant additional aspects of the mixed-alkali behaviour:

(i) The self diffusivity in a single-alkali glass is faster than foreign diffusivity in the same glass. This difference is much more pronounced when the minority ion has the larger ionic radius. Note, for example, that the Rb diffusivity on the Na-rich side is about four orders of magnitude slower than the Na diffusivity. On the other hand, the Na diffusivity on the Rb side is only about one order of magnitude slower than the Rb diffusivity.

(ii) The diffusivities of the two ions cross, when plotted as functions of the relative alkali content. This crossover occurs near the Na/(Na+Rb) ratio of the conductivity minimum (see Fig. 8). In addition, the crossover composition is almost independent of temperature.

(iii) Similar observations were reported, e.g., for Na-Rb germanate glasses [25], for Na-Rb silicate glasses [26], for Na-K silicate glasses [27], and for Na-Cs silicate glasses [28, 29].

One can define a 'hypothetical' average tracer diffusion coefficient as the weighted average of

the two tracer diffusivities. For Na-Rb borate glass we have

$$\langle D^* \rangle \;=\; XD^*(Na) + (1-X)D^*(Rb), \tag{5}$$

where $D^*(Na)$ and $D^*(Rb)$ denote the tracer diffusivities of ^{22}Na and ^{86}Rb. Note that this quantity is not directly accessible to experiments. A comparison between the average diffusivity with the charge diffusion coefficient D_σ is shown in Fig. 10 for Na-Rb borate glass with 20 mol % total alkali content. The crossover of the tracer diffusivities in mixed-alkali glass produces a minimum in $\langle D^* \rangle$, which is similar to that of the charge diffusion coefficient. The diffusivity crossover provides an approximate explanation for the mixed-alkali effect in the conductivity. The ratio $\langle D^* \rangle$ / D_σ can be used to deduce a common Haven ratio. The latter is smaller than unity and passes through a shallow maximum near the position of the conductivity minimum. The question remains why the diffusivities are so strongly composition-dependent.

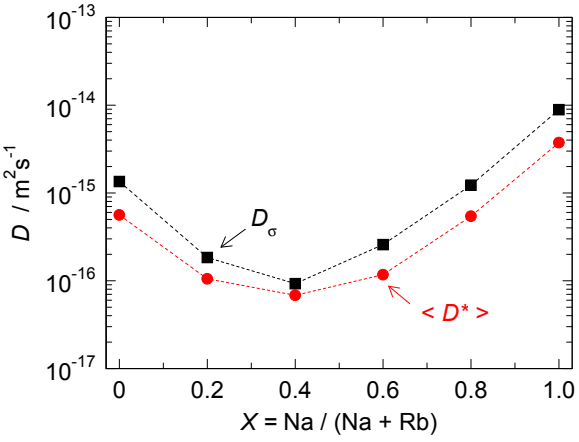

Figure 10. Comparison of the charge diffusion coefficient D_σ and of the average tracer diffusivity $\langle D^* \rangle$ for $0.2[X\mathrm{Na_2O}(1-X)\mathrm{Rb_2O}]\ 0.8\mathrm{B_2O_3}$ glasses at 300 °C.

A thorough understanding of the mixed-alkali effect is a long-standing challenge in glass science. In the authors' opinion the trend in the tracer diffusivities and the crossover behaviour is the key to an understanding of the MAE. Any model of the mixed-alkali effect must explain why the mobility of the majority ions can be significantly reduced by a small amount of minority ions. A commonly accepted explanation is still missing. Recent progress has been summarized elsewhere [17, 30, 31].

References

[1] Vogel W 1985 *Glass Chemistry* (Berlin: Springer)
[2] Shelby J E 1997 *Introduction to Glass Science and Technology* (The Royal Society of Chemistry, RSC paperbacks)
[3] Doremus R E 1994 *Glass Science* (New York: Wiley)
[4] Varshneya A K 1994 *Fundamentals of Inorganic Glasses* (Academic Press)
[5] Mehrer H 2007*Diffusion in Solids – Fundamentals, Methods, Materials, Diffusion-Controlled Processes* (Berlin: Springer)
[6] Tanguep-Njiokep E M and Mehrer H 2006 *Solid State Ionics* **177** 2839 - 2844
[7] Tanguep-Njiokep E M, Mehrer H and Imre A W 2007 *J. Non-Cryst. Solids* doi:10.1016/j.jnoncrysol.2007.07.045
[8] Imre A W, Voss S and Mehrer H 2002 *Phys. Chem. Chem. Phys.* **4** 3219 - 3224
[9] Mehrer H, Imre A W and Voss S 2003 in: CIMTEC 2002 – 3^{rd} Forum on New Materials, 2^{nd} Int. Conf. on *Mass and Charge Transport in Inorganic Materials*, Vincencini P and Buscaglia V (Eds.) (Techna Srl, Faenza) 127 - 138
[10] Imre A W, Voss S and Mehrer H 2004 *J. Non-Cryst. Solids* **333** 231 - 239
[11] Voss S, Imre A W and Mehrer H 2004 *Phys. Chem. Chem. Phys.* **6** 3669 - 3675
[12] Voss S, Berkemeier F, Imre A W and Mehrer H 2004 *Z. Physikalische Chemie* **218** 1353 - 1374
[13] Imre A W, Voss S and Mehrer H 2005 *Defect and Diffusion Forum* **237 - 240** 370 - 383
[14] Voss S, Divinski S V, Imre A W, Mehrer H and Mundy J N 2005 *Solid State Ionics* **176** 1383 - 1391
[15] Epping J D, Eckert H, Imre A W and Mehrer H 2005 *J. Non-Cryst. Solids* **351** 3521 - 3529
[16] Berkemeier F, Voss S, Imre A W and Mehrer H 2005 *J. Non-Cryst. Solids* **351** 3816 - 3825

[17] Imre A W, Divinski S V, Voss S, Berkemeier F and Mehrer H 2006 *J. Non-Cryst. Solids* **352** 783 - 788
[18] Imre A W, Voss S, Berkemeier F, Mehrer H, Konidakis H and Ingram M D 2006 *Solid State Ionics* **177** 963 - 969
[19] Imre A W, Berkemeier F, Mehrer H, Gao Y, Cramer C and Ingram M D 2007 *J. Non-Cryst. Solids* doi:10.1016/j.jnoncrysol.2007.07.087
[20] Imre A W, Staesche H, Voss S, Ingram M D, Funke K and Mehrer H 2007 *J. Phys. Chem.* B **111** 5301 - 5307
[21] Macdonald J R (Ed.) 1987 *Impedance Spectroscopy – Emphasizing Solid Materials and Systems* (John Wiley and Sons)
[22] Funke K, Banhatti R D, Brückner S, Cramer C, Krieger C, Mandanici A, Martiny C and Ross I 2002 *Phys. Chem. Chem. Phys.* **4** 3155
[23] Charles R J 1965 *J. Amer. Ceram. Soc.* **48** 432
[24] Gao Y and Cramer C 2005 *Solid State Ionics* **176** 921
[25] Estrop'ev K K and Pavlovsiki V K 1966 in: *Structure of Glass*, Porai-Koshits E A (Ed.) **7** (New York: Consultant Bureau)
[26] McVay G L and Day D E 1966 *J. Amer. Ceram. Soc.* **53** 508
[27] Fleming J W and Day D E 1972 *J. Amer. Ceram. Soc.* **55** 186
[28] Terai R 1971 *J. Non-Cryst. Solids* **5** 121
[29] Jain H, Peterson N L and Downing H L 1985 *J. Non-Cryst. Solids* **55** 2183
[30] Dieterich W and Maass P 2002 *Chem. Physics* **284** 439
[31] Bunde A, Dieterich W, Maass P and Meyer M 2005 *Ionic Transport in Disordered Materials*, Chap. 20 in: *Diffusion in Condensed Matter – Methods, Materials, Models*, Heitjans P and Kärger J (Eds.) (Berlin: Springer)